



Interfacial shear in downward two-phase annular co-current flow

M. Hajiloo^a, B.H. Chang^{b,*}, A.F. Mills^a

^a *University of California, Los Angeles, CA 90024-1597, USA*

^b *Inchon City College, Inchon 402-750, South Korea*

Received 16 November 1999; received in revised form 29 October 2000

Abstract

Pressure drop has been determined experimentally for downward co-current annular two-phase flow, with water and air flow Reynolds numbers in the ranges 5100–27 200 and 3400–21 600, respectively. In order to investigate the effect of tube diameter, four tubes, of I.D.'s ranging from 1.56–4.12 cm, were tested. Special care was taken to eliminate effects of surfactants. The resulting skin friction coefficients were only in qualitative agreement with most previously reported data. At a fixed gas Reynolds number, a large increase in friction accompanied a decrease in tube diameter. Existing correlations were found to be unsuccessful for the present data. © 2001 Published by Elsevier Science Ltd.

Keywords: Multi-phase flow; Annular flow; Vertical downward flow; Pressure drop; Interfacial shear stress

1. Introduction

There have been many studies of vertical two-phase annular flow, with upward flow of gas, and either an upward or downward flow of the liquid film on the tube wall. In contrast, there have been relatively few studies of the combination of downward flows of gas and liquid. The former combinations are encountered more often in engineering equipment, and also are characterized by critical flooding phenomena. However, the latter combination is also encountered in equipment, for example, in co-current gas scrubbers. In such equipment, pressure drop is often an important consideration, and thus the designer requires data for the friction factor (or, equivalently, the skin friction coefficient). In planning an experiment the gas and liquid flow rates are obvious parameters to be varied. In an early study, Bergelin et al. (1949) noted that waves on the liquid film act much like surface roughness in single-phase flow, causing increased friction due to form drag.

* Corresponding author.

Then, the ratio of a characteristic wave height to tube diameter should be an important dimensionless parameter affecting friction, indicating that diameter should be varied as an independent parameter. Chu and Dukler (1975) found that small capillary waves, rather than large amplitude gravity waves, were the major cause of increased form drag; thus, surface tension should also affect friction (as should the presence of surfactants).

In the few experimental studies of downward flow, attention has been focused on rather small areas of the parameter space, and a comprehensive and consistent data base is lacking. The present study was motivated by the need to design equipment for which (i) a clean water–air system is an appropriate model, (ii) liquid flow rates are relatively high (film Reynolds numbers in the range 5000–25 000), (iii) gas flow rates are relatively low (superficial gas flow Reynolds numbers in the range 5000–25 000), (iv) there is negligible liquid entrainment, and (v) tube diameter is an important design parameter. The specific objective was to obtain friction data for this area of the general parameter space.

Relevant experimental measurements of pressure drop in downward co-current flow are as follows. Bergelin et al. (1949) measured pressure drop in a 2.54 cm diameter, 3.3 m long tube, for superficial water and air Reynolds numbers of 0–10 000 and 3100–65 000, respectively. Their results were presented graphically and showed some friction coefficients lower than values expected for smooth wall, single-phase flow. Chien and Ibele (1964) measured pressure drop and mean film thickness in a 5.08 cm diameter, 3.2 m long tube for both the annular and annular-mist flow regimes, and water and air Reynolds number ranges of 1250–22 000 and 28 000–350 000, respectively. For the annular flow regime, the skin friction coefficient was correlated as

$$f = 0.92 \times 10^{-7} Re_G^{0.582} Re_L^{0.705}, \quad (1)$$

where $f = \tau_i / 0.5 \rho_G U_G^2$, $Re_G = U_G D / \nu_G$, $Re_L = U_L D / \nu_L$; τ_i is the interfacial shear stress, and the velocities are superficial values, determined as if the fluid in question flows alone in the test section. The superficial bulk gas velocity is thus $U_G = Q_G / (\pi D^2 / 4)$, where Q_G is the volume flow rate of gas and D is the tube diameter. Note that also, $Re_L = 4\Gamma / \mu_L$, is the usual film Reynolds number defined for falling films, where Γ is the mass flow rate per unit width of perimeter. Ueda and Tanaka (1974) measured pressure drop and film thickness in a 2.88 cm diameter, 1.825 m long tube for water and air Reynolds numbers of 185–13 500 and 6000–100 000, respectively. Their results are presented as plots of friction factor versus gas Reynolds number based on air velocity relative to the water surface velocity (taken to be 50% greater than the bulk value). Tishkoff et al. (1979) used a tube of 2.86 cm diameter, 1.83 m long, and presented plots of friction coefficient and mean film thickness versus air Reynolds number for $15800 < Re_G < 86400$ and $4040 < Re_L < 18690$. Effects of swirl generation of air and water on film thickness were also investigated. Chung and Mills (1974) studied gas absorption into falling films with co-current gas flow in a 2.03 cm diameter, 1.56 m long glass tube. Their results include plots of f versus Re_G for $0 < Re_L < 8030$ and $8000 < Re_G < 30000$. Fedotkin et al. (1979) measured pressure drop and film thickness in a 3 cm diameter, 2.38 m long tube for annular flow without liquid droplet entrainment, and the following correlation was suggested for $2000 < Re_L < 20000$ and $6000 < Re_G < 30000$.

$$\tau_i / (\mu_L^2 \rho_L g^2)^{1/3} = 1.35 \times 10^{-9} Re_L^{0.75} Re_G^{1.75}, \quad (2)$$

where g is acceleration due to gravity. With property values evaluated at 295 K, Eq. (2) becomes

$$f = 3.943 \times 10^{-3} Re_L^{0.75} Re_G^{-0.25}. \quad (3)$$

The results of these studies are summarized in Fig. 1. Ignoring the results of Fedotkin et al. (1979) for the present, we can say that the qualitative effects of liquid and gas flow rates are in general agreement. For a given tube diameter, f always increases with liquid flow rate. There is characteristic S-shaped variation of f with gas flow rate. For low liquid and gas flow rates f decreases with Re_G and approximates smooth wall single-phase behavior. At higher flow rates, f increases rapidly with Re_G , primarily due to wave induced form drag. At higher values of Re_G a maximum can be reached with a subsequent gradual decrease. The maximum is attributed to the onset of liquid entrainment by Chien and Ibele (1964), but Tishcoff et al. (1979) observed entrainment before the maximum in f was reached. In none of these prior studies was diameter varied as an experimental parameter, though the values used varied from 2.05 to 5.08 cm. Unfortunately, poor quantitative agreement between the results and insufficient overlap of parameter values precludes a satisfactory evaluation of the effect of diameter. Nevertheless, there is a general indication of a marked increase in f with decreasing tube diameter. The results of Fedotkin et al. (1979) are clearly inconsistent with the other studies. These workers state that their data are in qualitative agreement with those of Chien and Ibele (1964), but this contradicts the effect of diameter noted above. It was necessary to rely on a correlation given by Fedotkin et al. (1979) since the original data were not given in accessible form. Thus, it will not be profitable to give this study any further attention.

Since all the studies involved the water–air system, nothing can be deduced about the effect of fluid properties, in particular, surface tension. Different results can be expected for Freon refrigerants that have much lower surface tensions than does water. Furthermore, little attention has been paid to the possible effect of surfactants on the capillary waves, and hence on friction. The effect of surfactants on the behavior of water–air interfaces has been studied for many years. Surfactants are known to change surface properties, and to have a pronounced effect on the general characteristics of the interfacial wave structure. In studies of gas absorption into turbulent falling films, Chung and Mills (1974), Won and Mills (1982) and others have found that trace

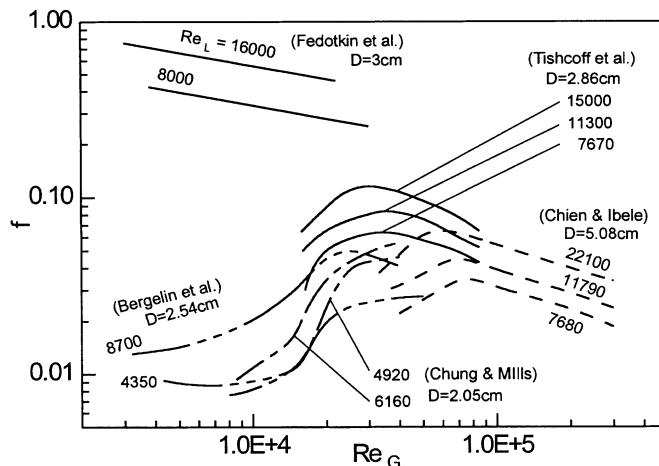


Fig. 1. Summary of previous work on downward co-current flow.

amounts of surfactants can appreciably affect gas absorption rates, a result that is attributed to the effect of the surfactants on capillary waves. In industrial equipment, surfactant introduced in the manufacturing and assembly stages is usually flushed out the system after days or weeks of operation. However, in laboratory experiments, tests have a relatively short duration and surfactant concentrations remain close to initial values. The ring test introduced by Crits (1961) is a simple and reliable test for determining if trace amounts of organic contaminants are present in water. This test proved indispensable in the gas absorption studies mentioned above, but has not seen much use in two-phase flow studies. It is possible that some of the inconsistency seen in Fig. 1 is due to different levels of surfactants, and in further experimental work it is essential to ensure that surfactants do not play a role.

2. Apparatus and procedures

In order to eliminate possible sources of organic contamination in the experiments, the use of oil, grease lubricated elements such as conventional water pumps, was avoided. The materials in direct contact with the water were restricted to glass, and easily accessible metal surfaces. Sealing was with Teflon seals, or Viton V14 O-rings. The experimental apparatus consists of two open loops, one for each phase. The water loop included activated charcoal filters, a constant level tank, a film distributor, the test section, and a collection tank on platform weigh scale. The distributor consisted of a 7° conical section which, by changing its height relative to the tube entrance, allowed the annular gap thickness to be easily adjusted. The schematic diagram of the annular film distributor is shown in Fig. 2. The gap thickness was set equal to the zero interfacial shear film thickness (evaluated from the correlation of Brotz, 1954) for the desired maximum water flow rate for the particular test tube.

The air loop consisted of rotary blower, a Rockwell-415 positive displacement gas flow meter, and an orifice plate system to calibrate the flow meter. The air temperature was monitored at the

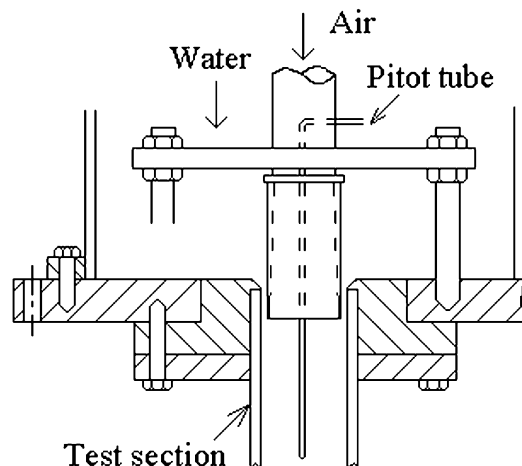


Fig. 2. Schematic diagram of the annular film distributor.

flow meter using a type K thermocouple, and air pressure at the meter and upstream of the test section were measured with single U-tube manometers. The static pressure drop was measured by a Hastings–Raydist inclinable manometer. Special care was taken to ensure that water did not become entrapped in the manometer connecting lines. The test sections were drawn glass tubes with inner diameters equal to 4.12, 3.42, 2.03 and 1.56 cm, and corresponding distances between static pressure taps of 1.77, 1.69, 1.34 and 1.24 m.

Prior to commencing testing, the system was thoroughly cleaned. Also, the accuracy of the platform scale was checked, and the gas flow-meter was calibrated. During the test program, the water was regularly subjected to the Crits (1961) organics ring test, and the activated charcoal filter packing replaced when necessary. The test procedure was straightforward: details are given by Hajiloo (1983). Bias errors in the flow rates and pressure drop are estimated to be no more than 3%. Using the method of Moffat (1988) the total uncertainty in the skin friction is estimated to be typically 9%.

3. Results

More than 250 data points were obtained for the four tube diameters, in the range $5070 < Re_L < 26700$ and $3390 < Re_G < 21400$. The ranges of superficial velocities were 0.32–0.78 m/s and 2.52–9.46 m/s for liquid and gas, respectively. These data are tabulated by Hajiloo (1983). Graphical results are presented first in terms of superficial quantities. Advantages of using superficial quantities include: (i) it eliminates the need to estimate the film thickness, (ii) it allows direct comparison between the present results and other experimental studies, and (iii) it allows easy use of the data for engineering calculations. In this scheme we define

$$U_G = 4Q_G/\pi D^2, \quad (4a)$$

$$U_L = 4Q_L/\pi D^2, \quad (4b)$$

$$Re_G = U_G D/\nu_G, \quad (4c)$$

$$Re_L = U_L D/\nu_L, \quad (4d)$$

$$f = 2\tau_i/\rho_G U_G^2, \quad (4e)$$

$$\tau_i = \left(\frac{\Delta P}{L} + \rho_G g \right) \frac{D - 2\delta}{4}, \quad (4f)$$

where ΔP is the pressure drop for a distance L between pressure taps. The mean film thickness δ was obtained from the following correlation of Henstock and Hanratty (1976).

$$\frac{\delta}{D} = \frac{6.59F}{(1 + 1400F)^{1/2}}, \quad (5a)$$

$$F = \gamma(\nu_L/\nu_G)(\rho_L/\rho_G)^{1/2} Re_G^{-0.9}, \quad (5b)$$

$$\gamma = \left[(0.707Re_L^{0.5})^{2.5} + (0.0379Re_L^{0.9})^{2.5} \right]^{0.4} \tag{5c}$$

The definitions in Eqs. (4a)–(4f) are equivalent to those used by earlier workers whose results are shown in Fig. 1. Tishkoff et al. (1979) and Chien and Ibele (1964) have used the Darcy friction factor that is four times the coefficient defined in Eq. (4e). The present results are shown in Fig. 3, where portions of the measured data have been excluded to avoid overcrowding the figure. The friction coefficient increases with liquid flow rate; it also generally increases with gas flow rate, except for high liquid flow rates in the 2.03 cm diameter tube for which f reaches a maximum and thereafter gradually decreases. Also, there is a marked increase in f with decreasing tube diameter.

One effect of increasing the liquid-phase flow rate is to produce thicker liquid films and a reduced cross-sectional area for the gas flow. An alternative method to present friction results is to base the gas velocity on the actual flow area. In this scheme the definitions used are

$$U_G^* = 4Q_G/\pi(D - 2\delta)^2, \tag{6a}$$

$$Re_G^* = U_G^*(D - 2\delta)/\nu_G, \tag{6b}$$

$$f^* = 2\tau_i/\rho_G U_G^{*2}. \tag{6c}$$

The results in Fig. 4 show that use of this scheme reduces the effect of Re_L . Also the effect of diameter is reduced, but remains large. For example, at $Re_G^* = 6000$ and $Re_L \approx 17000$, a reduction in tube diameter from 3.42 to 2.03 cm gives a 55-fold increase in f^* . It appears that use of the mean film thickness to correct the gas velocity does not properly account for the obstruction of the gas flow by the liquid film. Since the gas and liquid velocities are comparable at low gas flow rates, correlation of the present results using a friction factor based on relative velocity was attempted by Hajiloo (1983). This approach did not resolve the diameter effect, and it was abandoned.

The results of the present work in terms of superficial parameters are compared with those available from previous studies in Fig. 5. Though it is difficult to compare the individual results due to different pipe sizes, there seems to be a general qualitative agreement. For example, results

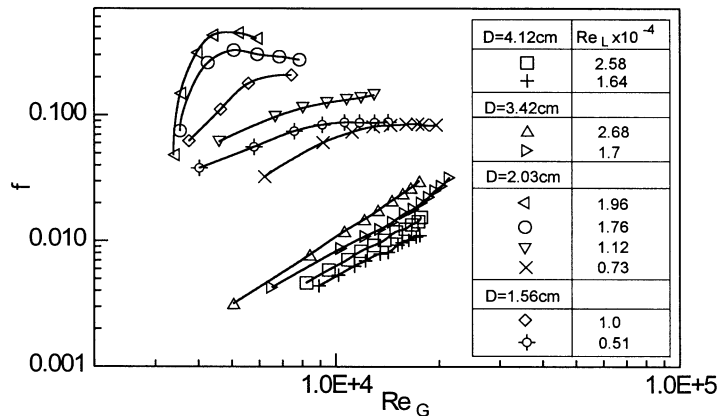


Fig. 3. Superficial friction coefficient versus superficial gas Reynolds number.

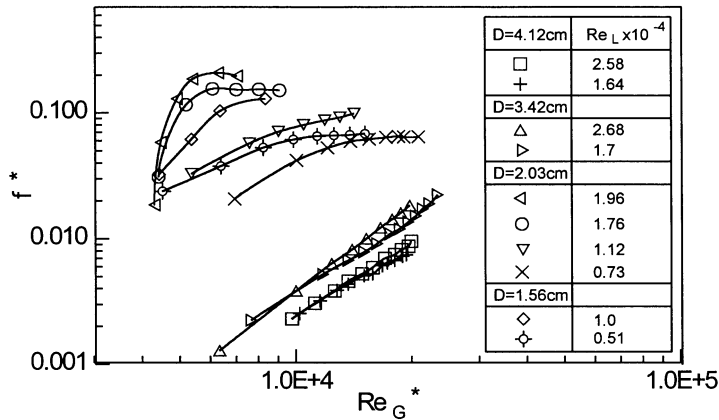


Fig. 4. Friction factor versus true gas Reynolds number.

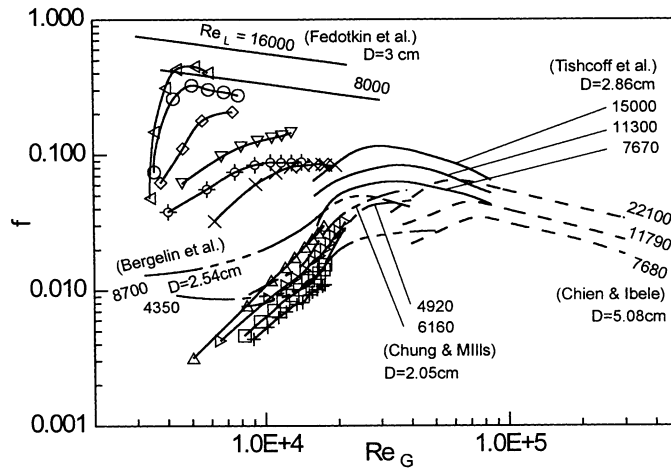


Fig. 5. Comparison of the experimental superficial friction factor with results of other investigators.

for Chien and Ibele (1964), Tishkoff et al. (1979), Bergelin et al. (1949), and present work show similar slopes for similar values of Re_L . Also, the results of Chien and Ibele (1964) can be extrapolated into the range covered by the present work for the larger diameter test sections.

The peaks occurring at high Re_L in the 2.03 cm tube (Figs. 3–5) are possibly due to incipient liquid entrainment. According to observations by Chien and Ibele (1964), the maximum friction factor occurs close, but prior to the onset of liquid entrainment. This is contrary to the experimental results of Tishkoff et al. (1979) who used a laser beam to detect liquid droplets and observed entrainment before the friction factor maxima. For the range of Re_L investigated, $4040 < Re_L < 18690$, Re_G at which the maximum friction factor occurs was almost twice larger than that at the onset of entrainment at around $Re_G = 20000$. No attempt was made in the present investigation to obtain data when entrainment was suspected because entrainment was undesirable in the design application motivating the work.

A factor that could affect comparisons of data from various studies is the effect of tube length. It appears that there are two opposing effects, namely (1) the development of waves, and (2) the development of the gas-phase velocity profile. Whereas the latter effect occurs over only about 15 tube diameters, the wave development can take a distance of the order of meters (Webb and Hewitt, 1975). Tishkoff et al. (1979) report a constant pressure gradient along a 1.83 m test section. Bergelin et al. (1949) report a lower pressure gradient near the entrance at low gas velocities, with a more linear behavior at the higher liquid flow rates used in our work: at high gas velocities the pressure gradient was found to be ‘remarkably linear’. Chien and Ibele (1964) used pressure gradients measured about 2 m from the inlet, whereas Bergelin et al. (1949) apparently measured an average pressure gradient over the last 5.5 m of a 6.1 m long tube. Our skin friction coefficients are based on average pressure gradients excluding the initial 5 cm from the water inlet. Further experimental work should clarify the variation of pressure gradient and hence the effect of tube length.

A number of friction correlations have been proposed by prior workers. In most cases, the emphasis has been on upward gas flows, but some recommendations have been made for co-current downward flows. Examples include correlations developed by Henstock and Hanratty (1976), Asali et al. (1985), Klausner and Chao (1991), and Fukano et al. (1991). None of these correlations were satisfactory for the present data. Nevertheless, it is useful to show their application to give some insights into the problem of developing a satisfactory correlation.

In their early work, Henstock and Hanratty (1976) present both explicit and implicit correlation forms. The explicit form is

$$f = f_s[1 + 1400F(1 - \exp(-A))], \quad (7a)$$

where

$$f_s = 0.046 Re_G^{-0.2}, \quad (7b)$$

$$A = [\rho_G U_G^2 f_s / \rho_L g D_h] \left[(1 + 1400F)^{1.5} / 13.2F \right] \quad (7c)$$

and F is defined by Eqs. (5b) and (5c). Application to the present data is shown in Fig. 6 to be quite unsuccessful. The implicit correlation of Henstock and Hanratty (1976) was also tested; although the data spread was somewhat reduced, it also was inadequate to handle the effect of tube diameter. The inadequacy with respect to tube diameter has already been noted by Asali et al. (1985), but based on results from different investigators. Here we have used results for a range of tube diameters from a single investigation to come to this conclusion.

Asali et al. (1985) recommend for the roll wave regime

$$f/f_s - 1 = 0.45 Re_G^{-0.2} (m_G^+ - 5.9), \quad (8a)$$

where

$$m_G^+ = 0.19 Re_L^{0.7} \frac{v_L}{v_G} \left(\frac{\rho_L \tau_i}{\rho_G \tau_c} \right)^{1/2} \quad (8b)$$

is a dimensionless film thickness, and τ_c is a characteristic shear stress that in terms of the interfacial value τ_i and wall value τ_w is

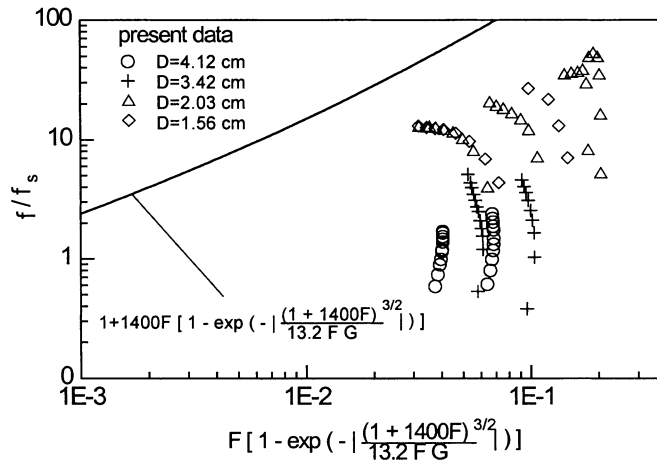


Fig. 6. Correlation of interfacial friction factor using Henstock and Hanratty (1976) method.

$$\tau_c = \frac{2}{3} \tau_w + \frac{1}{3} \tau_i. \tag{8c}$$

Fig. 7 shows the current data using the correlation of Asali et al. (1985) for the ripple regime, and the correlation is unable to account for the effect of tube diameter. The current data using the correlation for the roll wave regime, Eqs. (8a) and (8b), showed similar results as Fig. 7.

Klausner and Chao (1991) proposed a correlation based on published data of Webb (1970) and Andreussi and Zanelli (1978), and is

$$(f_c/f_s - 1) We^{1.5} = 9.15 \times 10^{-12} \delta_v^{+5.38}, \tag{9}$$

where the Weber number is defined as $We = \rho_L U_L^2 \delta / \sigma$, $\delta_v^+ = \delta (\tau_c / \rho_G)^{1/2} / v_G$ is a dimensionless film thickness based on the characteristic shear stress defined by Eq. (8c) and gas-phase properties, and

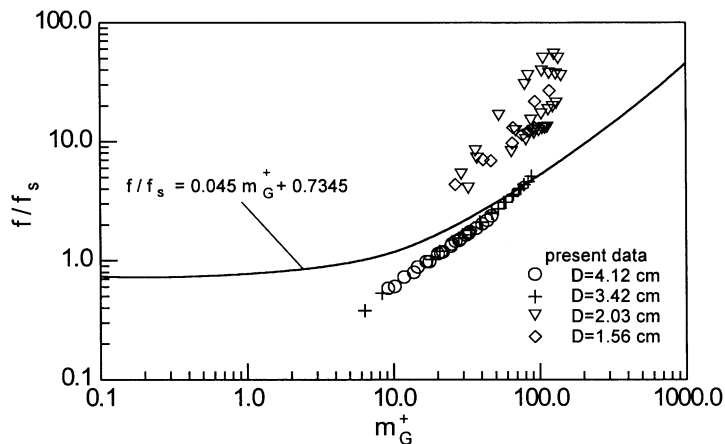


Fig. 7. Correlation of present data using Asali et al. (1985) ripple regime method.

$f_c = 2\tau_c/\rho_G U_G^2$. Fig. 8 shows that the correlation is relatively successful for the two larger tubes but not for the two smaller tubes: again the diameter effect is not properly accounted for.

The concept of waves on the liquid film acting like surface roughness in single-phase flow to increase friction has motivated these correlation schemes, leading to use of a dimensionless film thickness as a correlating parameter. For example, Henstock and Hanratty (1976) defined a dimensionless film thickness as the average film thickness divided by tube diameter. Asali et al. (1985) made the average film thickness dimensionless by forming a Reynolds number with the vapor friction velocity $(\tau_i/\rho_G)^{1/2}$ and vapor kinematic viscosity. Klausner and Chao (1991) replaced τ_i by τ_c in the Asali et al. (1985) definition. From the lack of success of these correlations it is apparent that the average liquid film thickness alone is not sufficient to characterize the effect of waves on friction. Other features of the wave structure, and the interaction of the gas flow with the wave structure, seem to play a role. The literature does contain some relevant information pertaining to wave structure. Chu and Dukler (1975) showed from their experimental-statistical study that the form drag caused by the large amplitude gravity waves never exceeded 4% for the total measured interfacial resistance. It was concluded that the small capillary waves on the interface was the primary contribution to the increased resistance to gas flow. Telles and Dukler (1970) showed that the ratio of rms fluctuation in film thickness to the mean film thickness increased with liquid flow rate and decreased with gas flow rate. Webb and Hewitt (1975) performed experiments with 3.18 and 3.82 cm diameter tubes and presented a flow regime map of ripple, dual wave, thick ripple, and regular wave regime. However, these results are for lower film Reynolds numbers than were the focus of this study. Definitive data on wave structure in the parameter ranges of concern are unavailable. A striking feature of the friction result is that increase over smooth wall values are far larger for two-phase flow than for rough wall single-phase flow. Referring to the 3.42 cm diameter tube for $Re_L = 26800$, Fig. 3 shows 10-fold increase in f as Re_G increases from 5050–17510, which is more than four times larger than comparable increases seen in Nikuradse (1933) sand-grain roughness friction data. Similarly, more than 50-fold increase in f with a diameter decrease of 3.42–2.03 cm, seen in Fig. 3, bears no relation to the less than two-fold increase seen for a similar diameter decrease in fully rough, single-phase flow. Clearly, the rough wall analog is

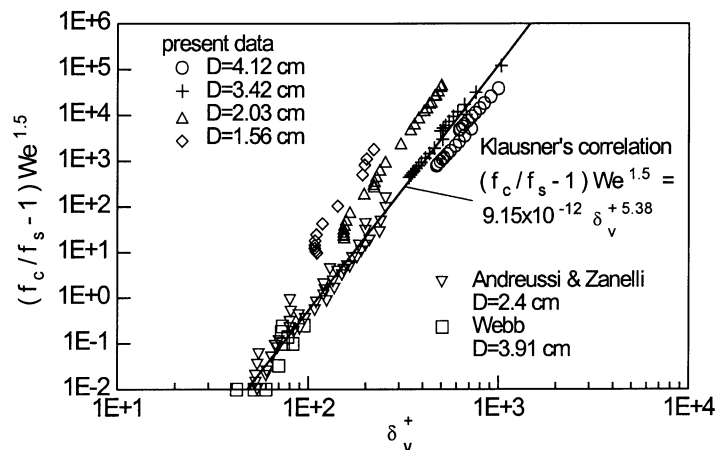


Fig. 8. Correlation of interfacial friction factor using Klausner and Chao (1991) method.

too simplistic to be of value in understanding friction in annular two-phase flow. We have not been able to develop a physics based correlation scheme for our friction data. For engineering use, numerical interpolation, or curve fitting in limited ranges of the parameter values, is recommended as a reliable approach. For this purpose Table 1 contains selected numerical data. If less accuracy is required, we have developed an empirical correlation of similar form to that of Asali et al. (1985), and is

$$f/f_s = 125.2m_G^{+1.51}Re_G^{-1.05}, \tag{10}$$

where m_G^+ is the dimensionless film thickness defined by Eq. (8b). The interfacial shear stress and the wall shear stress used in the correlation are

$$\tau_i = \left(-\frac{dP}{dx} + \rho_G g \right) \frac{D - 2\delta}{4}, \tag{11}$$

Table 1
Measured pressure gradients for the present experiment

<i>D</i> (cm)	<i>Re_L</i> (N/m ³)	<i>Re_G</i> (N/m ³)	$\Delta P/L + \rho_G g$ (N/m ³)	<i>Re_L</i> (N/m ³)	<i>Re_G</i> (N/m ³)	$\Delta P/L + \rho_G g$ (N/m ³)	<i>Re_L</i> (N/m ³)	<i>Re_G</i> (N/m ³)	$\Delta P/L + \rho_G g$ (N/m ³)
4.13	25753.	17716.	42.90	25753.	10822.	7.56	16386.	14201.	14.23
	25753.	17398.	38.01	25753.	9524.	4.89	16386.	13440.	12.45
	25753.	16643.	32.90	25753.	8199.	2.89	16386.	12164.	9.00
	25753.	15945.	28.01	16386.	17568.	29.34	16386.	11315.	7.11
	25753.	14970.	23.56	16386.	17149.	27.34	16386.	10169.	4.89
	25753.	13831.	17.34	16386.	16313.	23.34	16386.	8923.	3.11
	25753.	12912.	13.78	16386.	15587.	20.45			
	25753.	11824.	10.45	16386.	15131.	18.45			
3.42	26759.	17508.	142.94	26759.	8402.	8.95	17004.	16855.	77.51
	26759.	16543.	113.42	26759.	5053.	1.39	17004.	15885.	63.69
	26759.	15660.	91.81	17004.	21425.	220.81	17004.	14627.	46.14
	26759.	14550.	69.73	17004.	20344.	170.83	17004.	13444.	34.28
	26759.	13256.	48.81	17004.	19481.	144.10	17004.	12177.	24.87
	26759.	12103.	34.52	17004.	18660.	117.38	17004.	10364.	14.53
	26759.	10587.	21.38	17004.	17789.	96.46	17004.	6530.	2.91
2.03	19641.	5897.	1106.11	17593.	4255.	376.39	7289.	17874.	1889.61
	19641.	5207.	967.85	17593.	3536.	76.81	7289.	17309.	1797.43
	19641.	4390.	668.28	11248.	12926.	1751.35	7289.	16020.	1536.27
	19641.	3953.	399.43	11248.	11832.	1398.00	7289.	14429.	1229.01
	19641.	3539.	153.63	11248.	10744.	1113.79	7289.	12835.	952.49
	19641.	3389.	46.09	11248.	9410.	814.22	7289.	11137.	652.91
	17593.	7839.	1282.78	11248.	8029.	545.38	7289.	9177.	368.70
	17593.	6867.	1052.34	11248.	6666.	322.62	7289.	6218.	92.18
	17593.	5923.	829.59	11248.	4593.	99.86			
	17593.	5067.	660.60	7289.	19600.	2250.63			
1.56	9963.	7430.	1849.59	5067.	14195.	2737.06	5067.	9128.	1094.82
	9963.	5575.	912.35	5067.	12946.	2256.00	5067.	7569.	671.82
	9963.	4633.	398.12	5067.	11721.	1857.88	5067.	5795.	298.59
	9963.	3756.	149.29	5067.	10585.	1526.12	5067.	4017.	99.53

$$\tau_w = -\frac{dP}{dx} \frac{D}{4} + \rho_L g \frac{D}{4} \left(1 - \left(\frac{D - 2\delta}{D} \right)^2 \right) + \rho_G g \frac{D}{4} \left(\frac{D - 2\delta}{D} \right)^2. \tag{12}$$

Fig. 9 shows the present data correlated in this manner. Fig. 10 adds the data of Bergelin et al. (1949) and Chung and Mills (1974), and shows that these data are reasonably consistent with the present results. It must be cautioned that Eq. (10) is empirical and is simply a curve fit to the present data. It cannot be extrapolated outside the parameter range of our study, and cannot be used for liquids other than water.

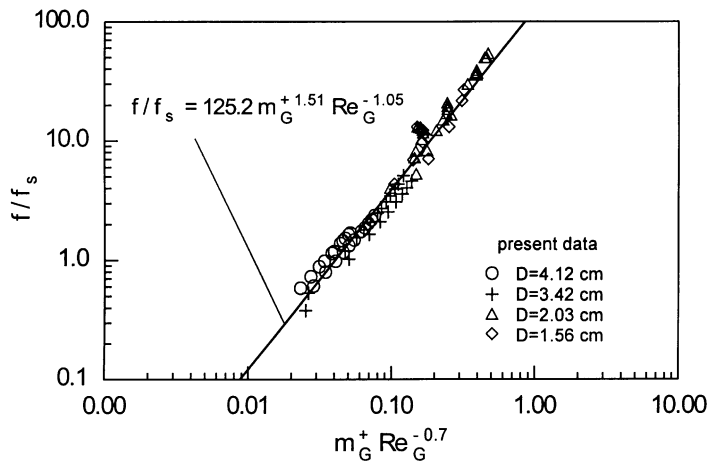


Fig. 9. Empirical correlation of the present data.

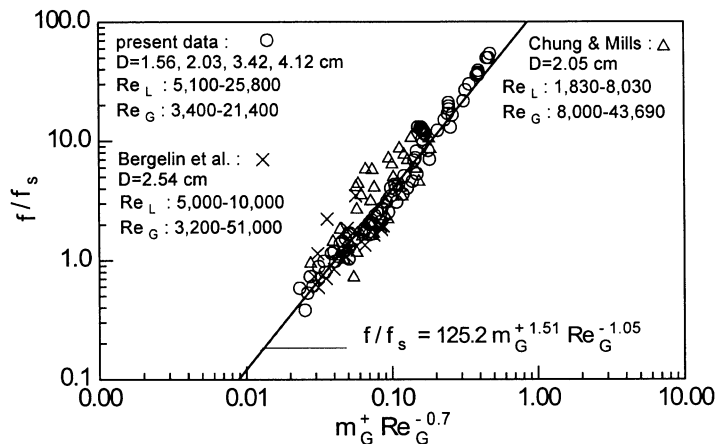


Fig. 10. Test of correlation using data of Bergelin et al. (1949) and Chung and Mills (1974).

4. Concluding remarks

New experimental data for friction in downward co-current two-phase flow has been obtained for water and air flow Reynolds numbers in the ranges 5100–27 200 and 3400–21 600, respectively. The data is unique in that the tube diameter was systematically varied from 4.13 cm down to 1.56 cm to demonstrate the critical importance of this parameter. Also, based on prior experience in performing experiments on gas absorption into falling water films, the experimental techniques ensured that organic surfactants were not present to affect the interfacial wave structure.

It was shown that there are large inconsistencies in the available data in this parameter range, and that available correlations are inadequate. The essential problems in correlating experimental data are (i) the data are not internally consistent, and (ii) the physics of why the presence of the liquid film has such a large effect on friction is not understood. Further progress requires more reliable data and a better understanding of the role played by the wave structure on the liquid film.

Acknowledgements

This work was supported in part by a grant from the Department of Energy through the Solar Energy Research Institute University Grants Program, Grant DE-FG02-SOCS89501.

References

- Asali, J.C., Hanratty, T.J., Andreussi, P., 1985. Interfacial drag and film height for vertical annular flow. *AICHE J.* 31, 895–902.
- Andreussi, P., Zanelli, 1978. Downward annular mist flow of air–water mixtures. International Seminar, Dubrovnik, Yugoslavia, 4–9 September.
- Bergelin, O.P., Kegel, P.K., Carpenter, F.G., Gazley, C. Jr., 1949. Co-current gas liquid flow. II. Flow in vertical tubes. *Heat Transfer and Fluid Mechanics Institute*, pp. 19–28.
- Brotz, W., 1954. Über die vorausberechnung der absorptions geschwindigkeit von gasen instramen den Flüssigkeitsschichten. *Chem. Eng. Tech.* 26, 470–478.
- Chien, S.F., Ibele, W., 1964. Pressure drop and liquid film thickness of two-phase annular and annular-mist flows. *J. Heat Transfer* 86, 89–96.
- Chu, K.J., Dukler, A.E., 1975. Statistical characteristics of thin, wavy films III. Structure of the large waves and their resistance to gas flow. *AICHE J.* 21, 583–593.
- Chung, D.K., Mills, A.F., 1974. Effect of interfacial shear on gas absorption into a turbulent falling film with co-current gas flow. *Lett. Heat Mass Transfer* 1, 43–48.
- Crits, G.J., 1961. Crits organic ring test. In: *Symposium on analytical methods with emphasis on minor elements*, Amer. Chem. Soc. Div. of Water and Waste Chemistry, Chicago, IL.
- Fedotkin, I.M., Ivanov, V.S., Lisman, V.S., Chepurnoy, M.N., Shnyder, V.E., 1979. Pressure drop in downtake turbulent film and gas flows. *Fluid Mech. – Sov. Res.* 8, 85–90.
- Fukano, T., Kawakami, Y., Qusaka, Akiharu, Tominaga, Akira, 1991. Interfacial shear stress and hold-up in an air–water annular two-phase flow. *ASME/JSME Thermal Eng. Proc.* 2, 217–222.
- Hajiloo, M., 1983. Experimental investigation of interfacial shear in downward, two-phase, annular, co-current flow with diameter effects. MS thesis, School of Engineering and Applied Science, University of California, Los Angeles.
- Henstock, W.H., Hanratty, T.J., 1976. The interfacial drag and the height of the wall layer in annular flows. *AICHE J.* 22, 990–1000.

- Klausner, J.F., Chao, B.T., 1991. An improved correlation for two-phase frictional pressure drop in boiling and adiabatic downflow in the annular flow regime. *Proc. Instn. Mech. Engrs.* 205, 317–318.
- Moffat, R.J., 1988. Describing the uncertainties in experimental results. *Exp. Thermal Fluid Sci.* 1, 3–17.
- Nikuradse, J., 1933. Laws of flow in rough pipes. English translation of VDI-Forschungsheft 361.
- Telles, A.E., Dukler, A.E., 1970. Statistical characteristics of thin, vertical, wavy, liquid films. *Ind. Eng. Chem. Fundam.* 9, 412–421.
- Tishkoff, J.M., Pinchak, A.C., Ostrach, S., 1979. Turbulent co-current gas–liquid flow in a tube with and without swirl. *J. Fluids Eng.* 101, 61–68.
- Ueda, T., Tanaka, T., 1974. Studies of liquid film flow on two-phase annular and annular-mist flow regions. *Bull. JSME* 17, 603–613.
- Webb, D., 1970. Studies of the characteristics of downward annular two-phase flow, 3. Measurements of entrainment rate, pressure gradient, probability distribution of film thickness and disturbance wave inception. AERE report R6426.
- Webb, D.R., Hewitt, G.F., 1975. Downwards co-current annular flow. *Int. J. Multiphase Flow* 2, 35–49.
- Won, Y.S., Mills, A.F., 1982. Correlation of the effects of viscosity and surface tension on gas absorption rates into freely falling turbulent liquid film. *Int. J. Heat Mass Transfer* 25, 223–229.